

## LOCAL MODELLING OF QUASIGEOID HEIGHTS WITH THE USE OF THE GRAVITY INVERSE METHOD – CASE STUDY FOR THE AREA OF POLAND

Marek TROJANOWICZ

*Institute of Geodesy and Geoinformatics, Wrocław University of Environmental and Life Sciences,  
Grunwaldzka 53, 50-357 Wrocław, Poland*

*Corresponding author's e-mail: marek.trojanowicz@igig.up.wroc.pl.*

*(Received September 2011, accepted March 2012)*

### ABSTRACT

This paper presents examples of application of the method of local quasigeoid modelling based on the geophysical technique of gravity data inversion, using non-reduced surface gravity data and GNSS/levelling height anomalies. Its capacity is demonstrated with three examples consisting in computing detailed local quasigeoid models for three areas situated in Poland. The test areas are different in size (3,900, 23,000, 117,000 sq. kilometres), in geographic location as well as in density of the gravity data coverage. For each of the test regions, calculations were done in three variants, viz. without using any global geopotential model and with application of EGM96 and EGM08 models. The obtained results indicate that the applied method is suitable for creating high accuracy local quasigeoid models (the accuracies obtained were at the level of accuracy of GNSS/levelling test data)

**KEYWORDS:** local quasigeoid model, gravity invers method, topographical mass density distribution model

### 1. INTRODUCTION

The inverse problem theory is widely described in the geophysical literature and the method of gravity data inversion is one of the fundamental techniques of geophysical interpretation of this data. Generally, the inverse method can be defined as determination of source parameters directly from gravity or magnetic measurements (e.g. Telford et al., 1990; Blakely, 1995; Tarantola, 2005). The fundamental equation of this method is written as follows (Blakely, 1995):

$$f(P) = \int_V S(Q)\psi(P,Q)dV \quad (1)$$

where  $f(P)$  is the potential field at  $P$ ,  $S(Q)$  describes the physical parameters of the source element at  $Q$ ,  $\psi(P,Q)$  is the function that depends on the location of the observation point  $P$  and the source element point  $Q$ ,  $V$  is the volume of the source.

Using equation (1) and given values of  $f(P)$  for a number of points, the geometric parameters of the source element  $V$  (nonlinear inverse problem) and some aspects of  $S(Q)$  (linear inverse problem) are determined (Blakely, 1995). For inversion of gravity data equation (1) is Newton's equation,  $V$  is the volume of mass that generates the field of gravity disturbances  $f(P)$ , and  $S(Q)$  is the function of mass density distribution.

Geodetic methods of geoid and quasigeoid modelling based on gravity data inversion concentrate

on solving integral equations of type (1), which is the Fredholm integral equation of the first kind. It must be emphasised that in geodesy mainly boundary integral equations are analysed, and a general description of such approach can be found in Heck (2003).

Geodetic studies concerned with geoid or quasigeoid modelling and the use the inverse problem of gravity data in the geophysical sense can be classified into two groups. On the one hand, there are studies that focus on the application of traditional methods of the geoid modelling in examination of density distribution of the Earth's crust masses (Vajda and Vaniček, 1997; 1999; 2002).

On the other hand, there are methods of local geoid and quasigeoid modelling where determination of density distribution of topographic or Earth's crust masses is the key step in the modelling process. Among these methods, the most common are the least square collocation method (LSC) and the point mass method. The LSC method, developed by Krarup (1969) with a Hilbert space approach and Moritz (1972) with a stochastic process approach, in the form of the least square collocation with parameters (Forsberg, 1984), also allows density estimation of topographic masses. This method may be regarded as a generalization of Nettleton's density profiling method to heterogeneous data (Forsberg, 1984). The point mass method may be considered as a specific example of a classical, geophysical inversion of gravity data, in which the searched point masses represent density distribution. Over the years, many variants of this method were developed. These

variants differ from each other mainly in determination of point mass locations (e.g. Brovar, 1983; Barthelmes and Kautzleben, 1983; Barthelmes and Dietrich, 1991; Lehmann, 1995). Comparison of this method with the collocation method for the Azores (Antunes et al., 2003) indicated a high accuracy of this approach, which is comparable to the collocation accuracy. This method was also applied to the geoid modelling in the Perth region of Western Australia (Claessens et al., 2001), where usefulness of this method for identification of areas with meaningful discrepancies in mass densities has been proved.

At this point, it should also be noted that the methods based on the variational methods have been intensively investigated in the last two decades. These methods use, for representation of the disturbing potential, functional bases generated in different ways, e.g. reproducing kernel or elementary potential functions. For details see Holota (1997a; 1997b; 1999; 2011).

The crustal masses density distribution model is also a key step in the quasigeoid modelling process in the technique, applications of which are discussed in this paper. This method was previously presented by Trojanowicz (2007) and is based on the linear inversion of gravity data. The outcomes of the quasigeoid modelling with the aforementioned method shows high accuracy and stability. This paper contains examples of application of this technique, as well as the results of analyses highlighting the benefits of this approach in the local modelling of the quasigeoid. The test calculations are referred to the area of Poland and compared to GNSS/levelling data and different previously developed quasigeoid models.

As reported in Kryński (2007), the first geoid model of the area of Poland was developed at the Institute of Geodesy and Cartography in Warsaw in 1961 on the basis of Astro-Geodetic deflections of the vertical and gravity anomalies. The accuracy of this model is estimated at the level of about  $\pm 60$  cm (Kryński, 2007). This model was twice revised (1970 and 1978) using new astronomical observations and more detailed gravity maps. Finally, its accuracy is estimated at  $\pm 30$  cm (Łyszkowicz, 1993). The first gravimetric geoid model, called "GEOID92", was developed at SRC (Space Research Centre, Polish Academy of Sciences) in 1992 (Łyszkowicz, 1993). This model was developed using gravity anomalies in the grid of  $5' \times 5'$  and the global geopotential model OSU86 (360, 360). Its accuracy is estimated at approximately  $\pm 10$  cm. In 1993, using the FFT technique a new geoid model called "geoid94" was elaborated (Łyszkowicz and Denker, 1994). In the calculations were used the same gravity data as previously and the global geopotential model OSU91A (360, 360). The same global geopotential model and set of gravity anomalies in the grid of  $1' \times 1'$  were used in the construction of a gravimetric

quasigeoid model "quasi95" (Łyszkowicz and Forsberg, 1995). Soon afterwards, by FFT method, another quasigeoid model ("quasi97b") was developed, based on free-air gravity anomalies in the grid of  $1' \times 1'$  and global geopotential model EGM96. The accuracy of this model was estimated at the level of  $\pm 5$  cm (Łyszkowicz, 1998). This model was the basis for later developed quasigeoid models: (unpublished) "GEOIDPOL' 2001" and (published) "GUGiK 2001" (Pażus et al., 2002). The accuracy of the latter model is estimated at the level of  $\mp 1.8$  cm (Kryński, 2007). Both models were formed by fitting the model "quasi97b" to the network of the measured GNSS/levelling height anomalies. Models "geoid94" and "GUGiK 2001" will be used later in this paper. The beginning of the XXI century is a period of intensive investigation on developing a 1 cm quasigeoid model for the territory of Poland. This work is concerned both with qualitative and quantitative analysis of data necessary to build a precise quasigeoid model as well as methods for its determination. The result of this study was the development of several new quasigeoid models, the newest „GDQ08” including, designed with the use of gravity data, deflections of the vertical and global geopotential model EGM08. Its accuracy is evaluated to be at the level of  $\mp 1.7$  cm (Kryński and Kloch-Główna, 2009).

In practice, each model of the gravimetric geoid and quasigeoid (viz. made only of gravity data) indicates a systematic offset and tilt in reference to GNSS/levelling data, caused by the long-wavelength errors of geoid or quasigeoid and systematic errors of both levelling and GNSS data (Tscherning, 2001; Łyszkowicz, 2000). Local or regional gravimetric models of geoid or quasigeoid are converted into GNSS/levelling geoid heights or height anomalies, often using advanced computation techniques (e.g. Fatherstone, 2000; Kryński, 2007). It becomes common to extend the scope of surveying data used for geoid and quasigeoid modelling with GNSS/levelling data. Moreover, the methods of geoid or quasigeoid modelling should also consider the possibility of determination of models fitted to the GNSS/levelling data. An approach to implementing this postulate is presented e.g. in Osada et al. (2005), and the results of the analysis in Kryński (2007). The method under investigation also satisfies this demand, using in the calculations free-air anomalies on the earth's surface or gravity disturbances and GNSS/levelling height anomalies.

## 2. DESCRIPTION OF THE APPROACH

Generally, the quasigeoid modelling problem using the Brun's formula may be replaced by the problem of disturbing potential modelling in the points on the Earth's surface and in the external space. This paragraph contains a description of the disturbing potential model and the way of estimating its parameters which have been delineated by Trojanowicz (2007).

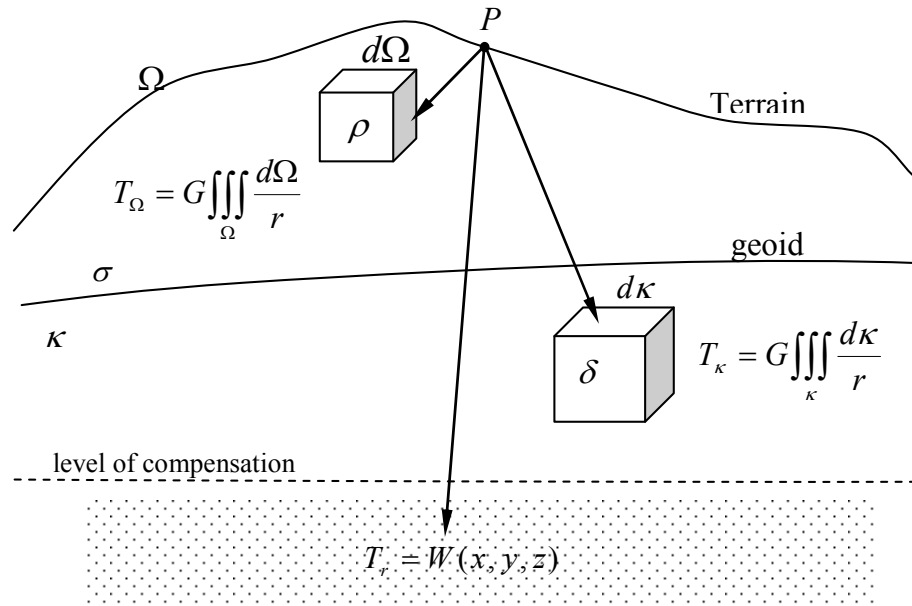


**Fig. 1** Disturbing potential model.

Let us consider a point  $P$  situated on a terrain surface (Fig. 1). The disturbing potential in this point can be split into three components:

- potential  $T_\Omega$  produced by topographic masses  $\Omega$  laying above the geoid, with density distribution function  $\rho$ .
- potential  $T_\kappa$  produced by disturbing masses  $\kappa$  occurring under the geoid surface, with density distribution function  $\delta$ .
- potential  $T_r$  which represents the remaining influences.

Potentials  $T_\Omega$  and  $T_\kappa$  produced by masses  $\Omega$  and  $\kappa$  are defined by Newton's integral and expressed respectively:

$$T_\Omega = G \iiint_\Omega \frac{\rho}{r} dV_\Omega \quad (2)$$

$$T_\kappa = G \iiint_\kappa \frac{\delta}{r} dV_\kappa \quad (3)$$

where  $G$  is the Newton's gravitational constant,  $dV_\Omega$  and  $dV_\kappa$  are elements of volume,  $r$  is the distance between the attracting masses and the attracted point  $P$ .

Regions  $\Omega$  and  $\kappa$  cover a limited areas of interest and for these areas the problem of inversion will be formulated. Parameters of the gravity field used as surveying data contain information about density anomalies also outside these areas. This unwanted part of the measurements should be filtered out (Forsberg, 1984). In the solution under analysis, the influence of the disturbing masses, which lay

outside the regions  $\Omega$  and  $\kappa$ , contain the potential  $T_r$ . Furthermore, its role is to link the gravity and the GNSS/levelling data, so that it has to model the offset and tilt between the gravimetric quasigeoid and GNSS/levelling data. For further calculations it was assumed that both the distorting effects mentioned can be modeled by harmonic polynomials of a low degree. This defines the form of the potential  $T_r$ .

Finally, the disturbing potential on the terrain surface can be written as:

$$T_p = T_r + T_\Omega + T_\kappa \quad (4)$$

Based on Eq. 4, we formulate a gravity inversion task as the one that requires: finding such functions of density distribution  $\rho$  and  $\delta$  inside the defined regions  $\Omega$  and  $\kappa$ , and polynomials coefficients of  $T_r$ , which satisfy the equality of the disturbing potential values given by equation (4) and its other quantities to their real values on the survey points.

Solution of the given task with the use of linear inversion, following Blakely (1995), requires discretization of the continuous 3D functions  $\rho$  and  $\delta$ . So, the regions  $\Omega$  and  $\kappa$  are divided into finite volume blocks and a constant density has to be assigned to each of the blocks. Densities of the blocks now become the searched values.

In the analyses referred to this paper we assumed that a zoning of the region  $\Omega$  is defined by a digital terrain model (DTM). Due to the fact that determination of the constant density for each DTM block involves calculation of too many unknown values, DTM blocks are grouped in the zones of the same density. So the searched, constant density  $\rho_k$

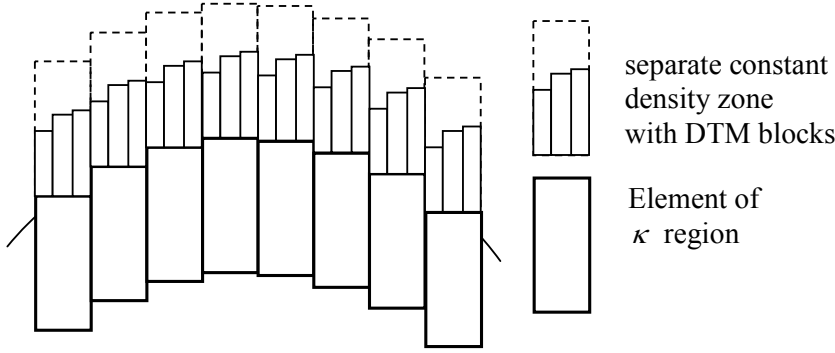


**Fig. 2**  $\Omega$  and  $\kappa$  regions in the Cartesian coordinate system.

refers to all DTM blocks situated in the  $k$  zone. The  $\kappa$  region may be treated as a slab of the same thickness. The division into blocks of constant density  $\delta_j$  would be the set consisting of one or many layers of spherical or rectangular prisms, depending on the adopted coordinate system. The speculations and analyses described in the successive part of this paper refer to the variant where it is assumed that the  $\kappa$  region has one layer whose thickness is nearly the same as the depth of the compensation surface. In the horizontal plane, the regions  $\Omega$  and  $\kappa$  go beyond the border of data occurrence. It should be noted that to solve the inversion of gravity data, just one layer of the searched densities is sufficient. This case, for the theoretical data model, was analysed with satisfactory results in the paper (Trojanowicz, 2002). However, when real data sets were used for this model, its accuracy became lower. Therefore, it was necessary to apply more layers, and as it transpires from the analysis, the usage of two layers provides very high accuracy with a minimal number of unknowns.

When the  $\Omega$  and  $\kappa$  regions are defined in such a way that the potential (4) may be described as a linear function of the searched parameters, which are  $\rho_k$  and  $\delta_j$ , and coefficients of the polynomial which approximates the  $T_r$  potential.

Calculations can be done using the spherical or Cartesian coordinate system. Detailed equations for both coordinate systems may be found in the paper Trojanowicz (2007). The below equations are for rectangular coordinates. These equations were applied to calculations the results of which are presented in the next part of this paper.

Let us introduce the Cartesian coordinate system. Its Z-axis is directed towards the geodetic Zenith and the X and Y axes lay on the horizontal plane and are directed to the North and East respectively. The origin of the coordinate system can be set in the middle of the area. In this case the  $\Omega$  and  $\kappa$  regions are defined as a rectangular grid of rectangular prisms (Fig. 2).

With  $\Omega$  and  $\kappa$  regions defined in this way, the potentials  $T_\Omega$  and  $T_\kappa$  can be represented as follows:

$$T_\Omega(P) = \sum_{k=1}^n \left( \rho_k G \sum_{i=1}^{m_k} \int_{z_{i1}}^{z_{i2}} \int_{y_{i1}}^{y_{i2}} \int_{x_{i1}}^{x_{i2}} \frac{1}{d_i} dx_i dy_i dz_i \right) = \mathbf{t}^T \mathbf{p} \quad (5)$$

where  $d_i = \sqrt{(x_i - X_p)^2 + (y_i - Y_p)^2 + (z_i - Z_p)^2}$ ,  $X_p, Y_p, Z_p$  - coordinates of point P,  $n$  - number of DTM zones (where for each zone the constant density  $\rho_k$  will be calculated),  $m_k$  - number of rectangular prisms of DTM in zone  $k$ ,  $x_{i1}, x_{i2}, y_{i1}, y_{i2}, z_{i1}, z_{i2}$  - coordinates defining rectangular prism  $i$  of DTM,  $\mathbf{p}^T = [\rho_1, \dots, \rho_n]$  is the vector of constant densities of topographic masses,  $\mathbf{t}^T = [t_1, \dots, t_n]$  comes from (5) and values  $t_k$  ( $k = 1 \dots n$ ) are defined as:

$$t_k = G \sum_{i=1}^{m_k} \left( \int_{z_{i1}}^{z_{i2}} \int_{y_{i1}}^{y_{i2}} \int_{x_{i1}}^{x_{i2}} \frac{1}{d_i} dx_i dy_i dz_i \right) \quad (6)$$

$$T_\kappa(P) = \sum_{j=1}^s \left( \delta_j G \int_{z_{j1}}^{z_{j2}} \int_{y_{j1}}^{y_{j2}} \int_{x_{j1}}^{x_{j2}} \frac{1}{d_j} dx_j dy_j dz_j \right) = \mathbf{r}^T \mathbf{\delta} \quad (7)$$

where  $d_j = \sqrt{(x_j - X_p)^2 + (y_j - Y_p)^2 + (z_j - Z_p)^2}$ ,  $s$  - number of rectangular prisms of the  $\kappa$  area,  $x_{j1}, x_{j2}, y_{j1}, y_{j2}, z_{j1}, z_{j2}$  - coordinates defining rectangular prism  $j$  of  $\kappa$  area,  $\mathbf{\delta}^T = [\delta_1, \dots, \delta_s]$  is the vector of constant densities of the region  $\kappa$ ,  $\mathbf{r}^T = [r_1, \dots, r_s]$  comes from (7) and values  $r_j$  ( $j=1 \dots s$ ) are defined as:

$$r_j = G \int_{z_{j1}}^{z_{j2}} \int_{y_{j1}}^{y_{j2}} \int_{x_{j1}}^{x_{j2}} \frac{1}{d_j} dx_j dy_j dz_j \quad (8)$$

**Note 1:** Equations (5-8) present topographic reduction, which should include the Earth's curvature. It entails designation of coordinates  $z$ , which define rectangular prisms of the regions  $\Omega$  and  $\kappa$  for each of the survey points. Let us assume a local, spherical model of the geoid. The coordinate  $z$ , which defines

either top or bottom surface of the rectangular prism  $i$  or  $j$  respectively, may be determined based on the height  $H$  of this surface above the geoid:

$$z = H - \left( R - \sqrt{R^2 - d_h^2} \right) \quad (9)$$

where  $R$  – mean radius of the Earth,  $d_h$  – horizontal distance of  $i$  or  $j$  block centre from the survey point

In the Cartesian coordinate system defined above, the direction of the  $Z$ -axis remains constant. The origin of the  $Z$ -axis is always under the actual survey point, at a depth equal to the height of the point. On account of this fact, the coordinate  $Z_p$  in equations (5-8) is equal to the height of the surveyed point  $H_p$  and may be replaced by this value.

As it was mentioned before, the potential  $T_r$  can be presented in the form of harmonic polynomials of a low degree. In the calculations the following polynomials were used (Brovar, 1983):

$$F(P) = a_1 + a_2 X_p + a_3 Y_p + a_4 X_p Y_p + a_5 Z_p = \mathbf{w}^T \mathbf{a} \quad (10)$$

where  $\mathbf{a}^T = [a_1, \dots, a_l]$  is the vector of the polynomial coefficients  $a_u$  ( $u=1\dots l$ ),  $\mathbf{w}^T = [w_1, \dots, w_l]$  comes from the form of the chosen polynomial

Solutions of the integrals in equations (5) and (8) and their vertical  $z$ -derivatives can be found in many publications (e.g. Forsberg and Tscherning, 1997; Nagy, 1966; Nagy et al., 2001).

Considering equations (5), (7) and (10), potential (4) can now be written as follows:

$$T_p = \mathbf{w}^T \mathbf{a} + \mathbf{t}^T \boldsymbol{\rho} + \mathbf{r}^T \boldsymbol{\delta} \quad (11)$$

Inversion of the gravity data is usually accomplished by adopting a certain reference density model, which can be described as  $\boldsymbol{\tau}_0^T = [\boldsymbol{\rho}_0^T, \boldsymbol{\delta}_0^T] = [\rho_1^0, \dots, \rho_n^0, \delta_1^0, \dots, \delta_s^0]$ . The searched values are not densities themselves but differences between real densities and the adopted reference model. Representing the density model as  $\boldsymbol{\tau}^T = [\boldsymbol{\rho}^T, \boldsymbol{\delta}^T] = [\rho_1, \dots, \rho_n, \delta_1, \dots, \delta_s]$ , the searched differences can be written as  $\mathbf{d}\boldsymbol{\tau}^T = \boldsymbol{\tau} - \boldsymbol{\tau}_0$ , and the vector of the unknown values as  $\mathbf{d}\mathbf{x}^T = [\mathbf{a}^T, \mathbf{d}\boldsymbol{\tau}^T]$ .

Taking it into account and assuming that the inversion problem can be solved using the least squares method, the relevant observation equations can be formulated. The basic survey data, according to the information in the introduction, are the values of the disturbing potential  $T_p$  obtained from GNSS/levelling height anomalies, as well as the gravimetric data in the form of free-air anomalies on the earth's surface  $\Delta g_p$  or gravimetric disturbances

$\delta g_p$ . For these data the observation equations are as follows:

$$\begin{aligned} T_p + v_{TP} &= \mathbf{f}^T \mathbf{d}\mathbf{x} + T_p^0 \\ \Delta g_p + v_{\Delta g_p} &= \left( -\mathbf{f}_z^T + \frac{U_{zz}}{\gamma_Q} \mathbf{f}^T \right) \mathbf{d}\mathbf{x} + \Delta g_p^0 \\ \delta g_p + v_{\delta g_p} &= -\mathbf{f}_z^T \mathbf{d}\mathbf{x} + \delta g_p^0 \end{aligned} \quad (12)$$

where  $\mathbf{f}^T = [\mathbf{w}^T, \mathbf{t}^T, \mathbf{r}^T] = [w_1, \dots, w_l, t_1, \dots, t_n, r_1, \dots, r_s]$  is the known vector,  $\mathbf{f}_z$  is the  $z$  derivative of the vector  $\mathbf{f}$ ,  $v_{TP}, v_{\Delta g_p}, v_{\delta g_p}$  are adjustment errors,  $\gamma_Q$  is a normal gravity acceleration on the telluroid and  $U_{zz}$  is its vertical gradient,  $T_p^0 = \mathbf{f}^T \mathbf{x}_0$ ,

$\Delta g_p^0 = \left( -\mathbf{f}_z^T + \frac{U_{zz}}{\gamma_Q} \mathbf{f}^T \right) \mathbf{x}_0$ ,  $\delta g_p^0 = -\mathbf{f}_z^T \mathbf{x}_0$  are the approximate observation quantities determined on the basis of the vector  $\mathbf{x}_0^T = [\mathbf{a}_0^T, \boldsymbol{\tau}_0^T]$ , where the vector  $\mathbf{a}_0$  is the  $l$ -dimension zero vector.

For a series of observations, the formulated equations (12), can be written in a more convenient form as:

$$\mathbf{v} = \mathbf{A}\mathbf{d}\mathbf{x} - \mathbf{L} \quad (13)$$

where  $\mathbf{v}^T = [v_{TP}, \dots, v_{\Delta g_p}, \dots, v_{\delta g_p}, \dots]$  is the vector of adjustment errors,  $\mathbf{L}^T = [T_p - T_p^0, \dots, \Delta g_p - \Delta g_p^0, \dots, \delta g_p - \delta g_p^0, \dots]$  is a known observation vector and  $\mathbf{A}$  is the design matrix of known coefficients.

With the given weight matrix  $\mathbf{P}$  (defined by the reciprocal of the observational errors squares), the system of equations (13) can be solved with the general condition of the least squares:

$$\mathbf{v}^T \mathbf{P} \mathbf{v} = \min \quad (14)$$

To overcome the non-uniqueness of the gravity inversion, the method suggested by Li and Oldenburg (1998) was used. It requires an additional condition to be put on the determined densities  $\mathbf{d}\boldsymbol{\tau}$ :

$$\mathbf{d}\boldsymbol{\tau}^T \mathbf{W}_\tau \mathbf{d}\boldsymbol{\tau} = \min \quad (15)$$

where  $\mathbf{W}_\tau$  is the model weighting matrix, the purpose of which is to strengthen or to weaken the influence of the designated values in various regions of the model domain on the data values.

Introducing the condition (15) gives a certain control over the inversion process. Recording this condition for the whole vector of the unknowns, the condition (15) may be written as:

$$\mathbf{d}\mathbf{x}^T \mathbf{W}_x \mathbf{d}\mathbf{x} = \min \quad (16)$$

where  $\mathbf{W}_x = \begin{bmatrix} \mathbf{W}_a & \mathbf{0} \\ \mathbf{0} & \mathbf{W}_\tau \end{bmatrix}$ , and  $\mathbf{W}_a$  is the zero model weighting matrix assigned to the vector of polynomial coefficients (10).

The model weighting matrix  $\mathbf{W}_\tau$ , which is presented in general form in Li and Oldenburg (1998), in order to serve the solution described in this paper, is defined as:

$$\mathbf{W}_\tau = \mathbf{W}^d + \mathbf{W}^c \quad (17)$$

where matrix  $\mathbf{W}^d$  is a diagonal matrix defined by the depth weighting function, whose elements are written as follows:

$$\mathbf{W}_{ii}^d = \begin{cases} \alpha_\Omega \sqrt{w_{\Omega k}} & \text{for } \Omega \\ \alpha_\kappa \sqrt{w_{\kappa j}} & \text{for } \kappa \end{cases} \quad (18)$$

where  $\alpha_\Omega$ ,  $\alpha_\kappa$  are constant coefficients and  $w_{\Omega k}$ ,  $w_{\kappa j}$  are equal to the value of the topographic correction for gravity, produced by zone  $k$  of constant density of the  $\Omega$  region or the cuboid  $j$  of region  $\kappa$ , at the point on the terrain surface, above the centre of the constant density zone  $k$  or cuboid  $j$ , matrix  $\mathbf{W}^c$  defines spatial correlations between zones of constant density and is defined as:

$$\mathbf{W}^c = \sum_{i=1}^n \sum_{p=3}^t \mathbf{C}^{ip} \quad (19)$$

where  $\mathbf{C}^{ip}$  is a matrix defining correlation between a couple of zones of constant density ( $i$ ,  $p$ ). In the matrix only four elements, corresponds to correlated zones ( $i$ ,  $p$ ), are not equal to zero and are defined as:

$$\begin{aligned} C_{ii}^{ip} &= w_i w_i, & C_{ip}^{ip} &= w_i w_p, \\ C_{pi}^{ip} &= w_p w_i, & C_{pp}^{ip} &= w_p w_p \end{aligned} \quad (20)$$

where  $w_i = -w_p = \beta \frac{\Delta x \Delta y}{d_{ip}^2}$ ,  $\beta$  is a constant coefficient,  $\Delta x$ ,  $\Delta y$  are mean distances between adjacent zones of constant density in  $x$  and  $y$  direction,  $d_{ip}$  is the distance between centers of zones  $i$  and  $p$ .

The least square objective function can now be written as:

$$\mathbf{v}^T \mathbf{P} \mathbf{v} + \mathbf{d} \mathbf{x}^T \mathbf{W}_x \mathbf{d} \mathbf{x} = \min \quad (21)$$

Equation set (13), including condition (21) is solved in the following way:

$$\mathbf{d} \mathbf{x} = (\mathbf{A}^T \mathbf{P} \mathbf{A} + \mathbf{W}_x)^{-1} \mathbf{A}^T \mathbf{P} \mathbf{L} \quad (22)$$

**Note 2:** Any inadequacy in the definition of known model parameters of the disturbing potential model

(4), like a lower resolution of the digital terrain model (DTM), division into zones of constant density which do not consider geological structures and borders of density changes, inadequate extent of the areas  $\Omega$  and  $\kappa$  or inappropriate form of the potential  $T_r$ , affects not only the estimated densities, but also the adjustment errors. Therefore, using a different way of designation of the matrices  $\mathbf{W}_x$  and  $\mathbf{P}$ , one can “locate” these inaccuracies in the model parameters, or in the adjustment errors. Hence, a proper designation of both matrixes is crucial for the final result of modelling.

In calculations, whose results are presented in this paper, to obtain matrix  $\mathbf{P}$  the height anomaly error was adopted at the level of the measurement errors. To estimate the errors of gravity data, the initial modelling procedure was used, in which the weights of gravity data were assumed very small, in order not to limit the estimated parameters of the model (in the calculations the error of gravity data  $m_{\delta g} = \pm 10 \text{ mGal}$  was used). Then the standard deviation of the adjustment errors of gravity data was estimated. This value was taken as gravity data errors in the successive main calculations. In order to determine the optimal values the coefficients  $\alpha_\Omega$ ,  $\alpha_\kappa$ , and  $\beta$ , separate analyzes were conducted, results of which are presented in the paper Trojanowicz (2012). The present calculations were carried out using the following values of the coefficients:  $\alpha_\Omega = 0.01$ ,  $\alpha_\kappa = 0.1$ ,  $\beta = 0.0015$ .

**Note 3.** Currently, geoid and quasigeoid modelling are commonly implemented using the global geopotential models. In the presented approach, the global geopotential models were used in the remove-compute-restore technique. So, the disturbing potential is presented as a sum of the global component  $T_{GM}$  (from the used global geopotential model) and residual potential  $T_{\Delta g}$  ( $T = T_{GM} + T_{\Delta g}$ )

.The calculations are carried out in three stages:

1. The global component is removed from the measured data. In this way, the residual data are formed:  $T_{\Delta g} = T - T_{GM}$  for GNSS/leveling and  $\delta g_{\Delta g} = \delta g - \delta g_{GM}$  for gravity disturbances.
2. Based on the residual data, a model of residual disturbing potential is build. From this model at the new points the residual disturbing potential values are determined.
3. Global component is restored at the new points:  $T = T_{GM} + T_{\Delta g}$

Considering the above, densities are also decomposed into two components  $\rho = \rho_{GM} + \rho_{\Delta g}$  and  $\delta = \delta_{GM} + \delta_{\Delta g}$ . The components  $\rho_{GM}$  and  $\delta_{GM}$  are estimated based on the data  $T_{GM}$  and  $\delta g_{GM}$ , whereas the components  $\rho_{\Delta g}$  and  $\delta_{\Delta g}$  are determined based on

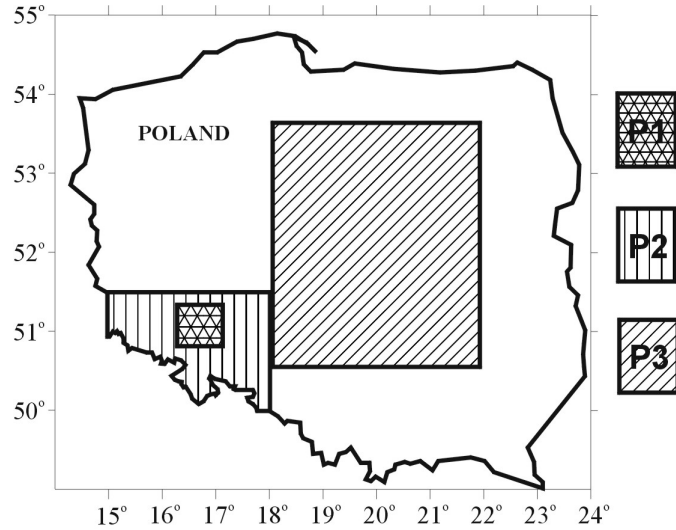


**Fig. 3** Test regions.

the data  $T_{\Delta g}$  and  $\delta g_{\Delta g}$ . Different reference density models ( $\rho_0, \delta_0$ ) can be used for both the mentioned steps of density modelling. This gives the possibility to implement in calculations various procedures for using the reference density models as well as various upper layers of the Earth's crust density models.

The above notes indicate clearly that the presented method is not yet in the closed form and requires further studies. The guidelines of these studies should certainly focus in the first place on the problem of designation of the matrixes  $\mathbf{P}$  and  $\mathbf{W}_x$  as well as estimation and use of the reference density models  $\rho_0, \delta_0$ .

### 3. TEST CALCULATIONS

Test calculations were carried out for three test areas situated in Poland. These areas are presented in Figure 3.

For all the test regions, in calculations of the elements of the model weighting matrix (17), a unit density of mass was assumed.

The reference density model was defined in the following way:

For components  $\rho_{\Delta g}$  and  $\delta_{\Delta g}$ , constant value  $\rho_0 = 2200 \text{ kg/m}^3$  (value close to the mean density of topographic masses for lowland areas of Poland (Królikowski and Polechońska, 2005)) as the reference density model for the area  $\Omega$  was assumed. Reference density model for the area  $\kappa$  ( $\delta_0$ ) was adopted as negative density, which balanced topographical masses of the area  $\Omega$ . So the density of separate prism of the area  $\kappa$  was calculated based on

the equation  $\delta_j^0 = -\frac{H_i \rho_i^0}{h_j}$ , where  $H_i, \rho_i^0$  are mean

height and reference density of the zone  $i$  of the  $\Omega$  area, situated directly above prism  $j$  of the area  $\kappa$ . For modelling of the components  $\rho_{GM}$  and  $\delta_{GM}$  the values  $\rho_0 = 0, \delta_0 = 0$  were adopted as reference density model.

The following parts of this paragraph contain description of the test regions and results of the calculations.

#### 3.1. TEST REGION P1

The test region P1 covers the central part of Lower Silesia. It is mostly a lowland and flat area. Only its south-western part covers the tectonic Sudetes foreland. Calculations were done in a local rectangular coordinate system whose origin is at the point  $\varphi = 51^\circ 6'$ ,  $\lambda = 16^\circ 30'$ . The area is presented in Figure 4.

For the purpose of calculations, 471 gravity points<sup>1</sup>, covering the area of ca.  $63 \times 62 \text{ km}$  (1 point per approx. 8 square kilometres) were used (Fig. 4). For this area, there are not enough points with known GNSS/levelling height anomalies, which could be used as data (known) points and test points. For the purpose of analysis, the quasigeoid model developed for the area of Poland, mentioned in Introduction as "GUGiK 2001", was used. Height anomalies determined for this model will be denoted as  $\zeta_{GUGiK}$ . From the model, the quasigeoid heights were determined in 9 points treated as data points and 273 test points, which are evenly distributed over the area,

<sup>1</sup> Data referred to the International Gravity Standardization Network 1971 (IGSN71), provided by the Polish Geological Institute.

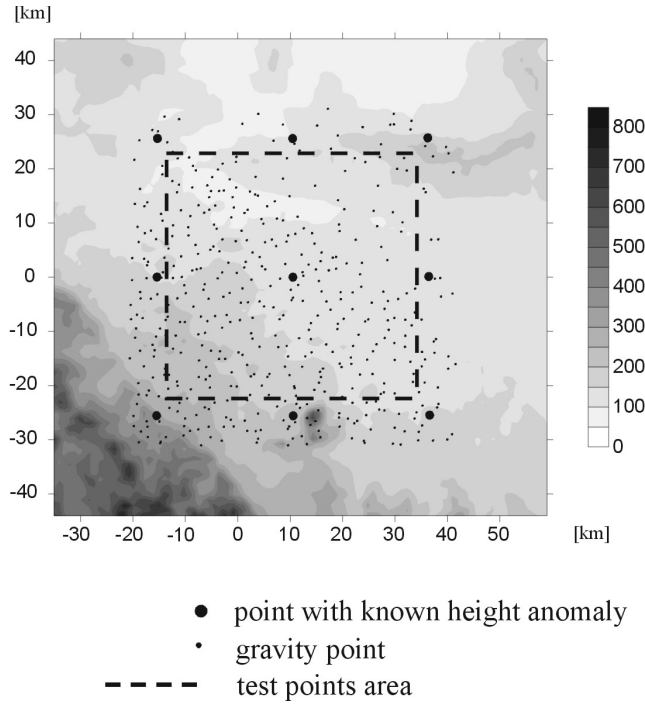


**Fig. 4** Test region P1.

**Table 1** Comparison of height anomalies determined with the analysed method and from global geopotential models EGM96 and EGM08 with their “theoretical” values.

	<i>min</i>	<i>max</i>	<i>RMS</i>	$\sigma$	<i>unit</i>
$d_{\zeta_{M0}}$	-1.61	1.56	$\pm 0.67$	$\pm 0.65$	cm
$d_{\zeta_{M96}}$	-1.36	1.00	$\pm 0.55$	$\pm 0.48$	cm
$d_{\zeta_{M08}}$	-1.23	1.33	$\pm 0.52$	$\pm 0.48$	cm
$\zeta_{EGM96} - \zeta_{GUGiK}$	-10.6	35.3	$\pm 14.0$	$\pm 11.9$	cm
$\zeta_{EGM08} - \zeta_{GUGiK}$	-4.0	3.1	$\pm 1.3$	$\pm 1.30$	cm

whose border is marked in Figure 4 with dashed line. In calculations was used the digital elevation model<sup>2</sup> with the resolution of 1000×1000 m, covering an area of 88×95 km. The region was divided into 900 zones of constant density of topographic masses. A particular zone was a rectangle with the size of ca. 2.9×3.2 km. The  $\kappa$  region was defined as a set of rectangular prisms that constitute a layer that has constant thickness of 32 km (the approximate depth of the compensation surface in the Lower Silesia region (Fajkiewicz, 1972)). Single cell of the  $\kappa$  region corresponded to the appropriate zone of the  $\Omega$  region by its horizontal size and position.

Calculations were done in three variants, viz. without the use of any global geopotential model and applying global models EGM96 (Lemoine et al.,

1998) and EGM08 (Pavlis et al., 2008). Results are presented as differences  $d_{\zeta}$  (in centimetres) between quasigeoid heights calculated from the model and its “theoretical” ( $\zeta_{GUGiK}$ ) values. Table 1 includes basic statistics of the differences. The following symbols were used for particular variants:  $d_{\zeta_{M0}} = \zeta_{M0} - \zeta_{GUGiK}$ ,  $d_{\zeta_{M96}} = \zeta_{M96} - \zeta_{GUGiK}$ ,  $d_{\zeta_{M08}} = \zeta_{M08} - \zeta_{GUGiK}$ .

To indicate high variability of the quasigeoid shape on the test area, and to estimate impact of the geopotential model quality on the calculation results, Table 1 presents also basic statistics of discrepancy between height anomalies calculated from the global models EGM96 ( $\zeta_{EGM96}$ ) and EGM08 ( $\zeta_{EGM08}$ ) and the “GUGiK 2001” model.

<sup>2</sup> Model built on the basis of the GTOPO30 model, available at the website of the Earth Resources Observation and Science (EROS) Center. This model was used in all calculations.

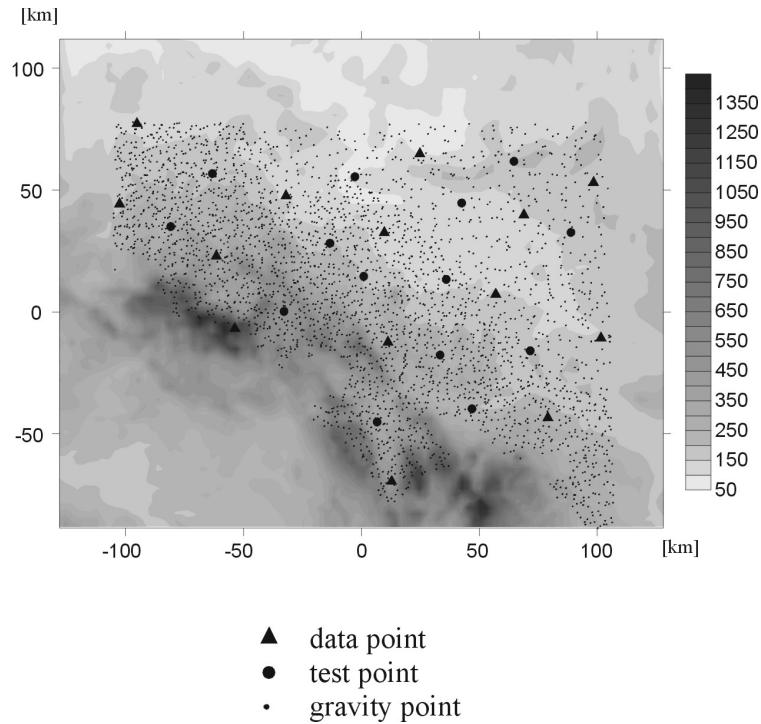


**Fig. 5** Test region P2.

**Table 2** Comparison of height anomalies determined with the analysed method and from global geopotential models EGM96 and EGM08 with GNSS/levelling data.

	<i>min</i>	<i>max</i>	<i>RMS</i>	$\sigma$	<i>unit</i>
$d_{\zeta_{M0}}$	-2.9	4.5	$\pm 2.3$	$\pm 2.1$	cm
$d_{\zeta_{M96}}$	-2.6	4.4	$\pm 1.7$	$\pm 1.5$	cm
$d_{\zeta_{M08}}$	-3.5	3.3	$\pm 1.6$	$\pm 1.6$	cm
$\zeta_{EGM96} - \zeta_{SL}$	-8.8	41.1	$\pm 20.8$	$\pm 15.0$	cm
$\zeta_{EGM08} - \zeta_{SL}$	-5.6	5.5	$\pm 2.7$	$\pm 2.4$	cm

### 3.2. TEST REGION P2

The test region P2 covers the whole Lower Silesia. The north-east part of this region is flat. The south-west covers the tectonic Sudetes foreland and the Sudetes mountains with the highest peak of 1602 m a.s.l. Calculations were done in a local rectangular coordinate system, with origin at  $\varphi = 50^{\circ}48'$ ,  $\lambda = 16^{\circ}30'$ . This area is presented in Figure 5.

As data set for calculations, 1518 gravimetric points<sup>3</sup> were used, covering an area of approx.  $23,000 \text{ km}^2$  (1 point per approx. 15 square kilometres) and 28 points of the POLREF network<sup>4</sup>. For the points of the POLREF network

GNSS/levelling height anomalies ( $\zeta_{SL}$ ) have been designated with the accuracy estimated at the level of  $\pm 2 \text{ cm}$  (Kryński et al., 2005). This accuracy was later found to be too optimistic, and estimated at the level of 3-4 cm (Kryński, 2007). The points were separated into two groups. The first group consists of 14 points treated as data points, which are represented in the Figure 5 by triangles. The remaining 14 points, marked in Figure 5 with larger dots, constitute the second group, which is a test group. Distances between adjacent, known points are in the range of approx. 30-70 km, and the mean distance is about 45 km. The digital terrain model used in the calculations, with resolution of  $1000 \times 1000 \text{ m}$ , covers

<sup>3</sup> Data referred to the International Gravity Standardization Network 1971 (IGSN71), provided by the Polish Geological Institute.

<sup>4</sup> POLish Reference Frame - data provided by the Head Office of Geodesy and Cartography of Poland.

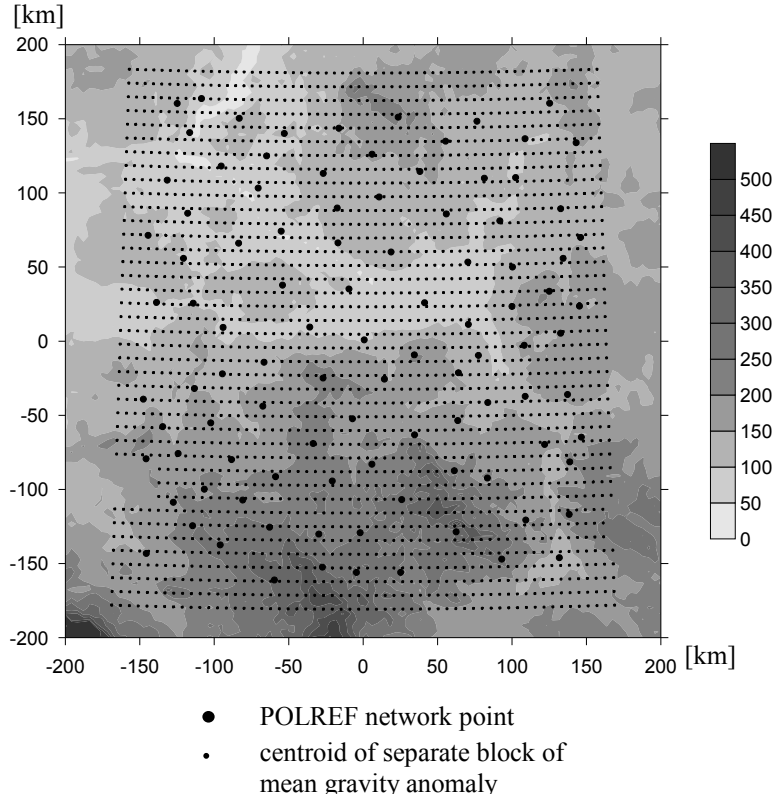


**Fig. 6** Test region P3.

the area of  $201 \times 256$  km. The region was divided into 900 zones of constant density of topographic masses. A particular zone was a rectangle of ca.  $6.7 \times 8.5$  km. The rule of defining the  $\kappa$  region remained the same as for the test region P1.

As in the previous example, calculations were done in three variants (without use of any global geopotential model and applying the global models EGM96 and EGM08). For each variant the differences between quasigeoid heights from the model and the measured GNSS/levelling height anomalies ( $\zeta_{SL}$ ) were calculated. The differences are marked as  $d_{\zeta_{M0}} = \zeta_{M0} - \zeta_{SL}$ ,  $d_{\zeta_{M96}} = \zeta_{M96} - \zeta_{SL}$ ,  $d_{\zeta_{M08}} = \zeta_{M08} - \zeta_{SL}$  and their basic statistics are presented in Table 2. The Table includes also basic statistics of the discrepancies between height anomalies calculated from the used global geopotential models and the  $\zeta_{SL}$  values.

### 3.3. TEST REGION P3

Test region P3 covers the central part of Poland. The region is formed mostly of lowlands and flatlands. Only in its southern part, there are highlands (Kielce Highland, the Kraków-Częstochowa Jurassic Highland Chain). Calculations were done in a local, rectangular coordinate system, origin of which is at the point  $\varphi = 52^\circ$ ,  $\lambda = 20^\circ$ . This area is presented in

Figure 6. In the calculations, 2302 mean free air anomalies<sup>5</sup> (Fig. 6) in the grid of  $5' \times 5'$  covering the area of approx.  $117,000$  km<sup>2</sup> (the single block has the size of approx.  $53$  km<sup>2</sup>) were used, as well as 100 points of the POLREF network situated in this area.

The digital terrain model used in calculations was of  $1000 \times 1000$  m resolution and covered the area of  $400 \times 400$  km. The region was divided into 900 zones of constant density of topographic masses. A particular zone was a rectangle of ca.  $13.3 \times 13.3$  km size. Despite the fact that the depth of the Moho discontinuity in the area oscillates from 42-47 km in the north-east part (Precambrian East European platform), about 50 km in the strip of land from the north-west to the south-east (Teisseyre-Tornquist Zone), to 32-36 km in the south-west part (Caledonides and Variscides), the principles of defining the  $\kappa$  region remain the same as for the other examples.

As previously, calculations were done in three variants. Results of calculations are presented using the same symbols as in the test area P2.

As the first test, a series of 100 calculations were taken. In each calculation set, one of the POLREF points was taken as the unknown and the other 99 points were treated as data points. Such approach was implemented to assure a minimal distance between

<sup>5</sup> Data in the Potsdam system referring to GRS80 ellipsoid were available at the website of the International Gravimetric Bureau

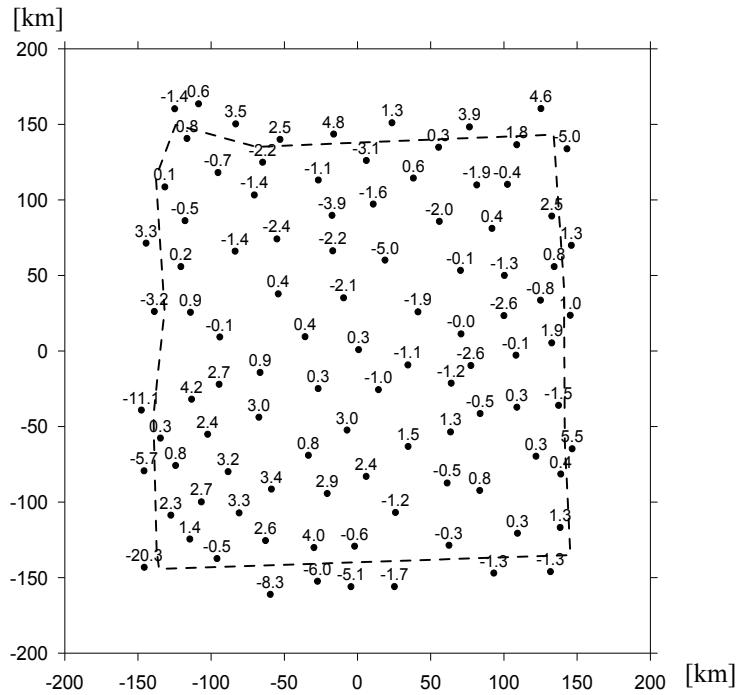


Fig. 7 The differences  $d_{\zeta_{M0}}$ , in centimetres.

Table 3 Comparison of height anomalies determined with the analysed method and from global geopotential models EGM96 and EGM08 with GNSS/levelling data.

	<i>min</i>	<i>max</i>	<i>RMS</i>	$\sigma$	<i>unit</i>
$d_{\zeta_{M0}}$	-5.1	4.2	$\pm 1.9$	$\pm 1.9$	cm
$d_{\zeta_{M96}}$	-3.1	3.6	$\pm 1.3$	$\pm 1.3$	cm
$d_{\zeta_{M08}}$	-3.9	3.7	$\pm 1.6$	$\pm 1.6$	cm
$\zeta_{EGM96} - \zeta_{SL}$	-20.1	28.4	$\pm 10.9$	$\pm 10.7$	cm
$\zeta_{EGM08} - \zeta_{SL}$	-7.7	4.8	$\pm 3.4$	$\pm 3.0$	cm

unknown and known points. Distances between known points are in the range of approx. 26-75 km, and a mean distance is about 52 km. The largest differences  $d_{\zeta_{M0}}$ ,  $d_{\zeta_{M96}}$ ,  $d_{\zeta_{M08}}$  appear at points situated close to the border of the elaboration area (Figure 7 shows  $d_{\zeta_{M0}}$  values as an example). The reduction in accuracy of the height anomalies determination near the border of the elaboration area (the edge effect) is the expected phenomenon and it reaches the largest values for the M0 variant.

The area where the edge effect is significant is separated by a dashed line in Figure 7 and constitutes the external part of the whole elaboration area. The internal part defines a certain sub-area (the efficiency area), in which the calculated height anomalies are very close to their “theoretical” values. Points situated inside the efficiency area are used for estimating the precision of the method.

In Table 3 the basic statistics of the differences  $d_{\zeta_{M0}}$ ,  $d_{\zeta_{M96}}$ ,  $d_{\zeta_{M08}}$ , calculated on the basis of 77 POLREF network points lying within the efficiency area, is presented.

For comparison, Table 4 includes the calculated, based on the same 77 test points situated inside the efficiency area, statistics of accuracy of two geoid and quasigeoid models obtained by classical, established approaches. The first is the geoid model „geoid94”. Because there exists a bias and a tilt between GNSS/levelling data and the “geoid94” model, Table 4 includes statistics for values which do not take into account a bias and a tilt ( $\zeta_{geoid94}$ ), and after the local designation of the bias and the tilt, based on all test points ( $\zeta_{geoid94}^*$ ). Height anomalies were derived from the geoid model with the use of the

**Table 4** Comparison of GNSS/levelling height anomalies with height anomalies determined from the models "geoid94" and "GUGiK 2001".

	<i>min</i>	<i>max</i>	<i>RMS</i>	$\sigma$	<i>unit</i>
$\zeta_{geoid94} - \zeta_{SL}$	-10.8	10.2	$\pm 5.5$	$\pm 4.8$	cm
$\zeta_{geoid94}^* - \zeta_{SL}$	-5.8	6.1	$\pm 2.8$	$\pm 2.8$	cm
$\zeta_{GUGiK} - \zeta_{SL}$	-5.4	1.4	$\pm 1.9$	$\pm 1.4$	cm

**Table 5** Basic statistics of differences  $d_{\zeta_{M075}}$ ,  $d_{\zeta_{M9675}}$ ,  $d_{\zeta_{M0875}}$ .

	<i>min</i>	<i>Max</i>	<i>RMS</i>	$\sigma$	<i>unit</i>
$d_{\zeta_{M075}}$	-7.1	7.4	$\pm 3.4$	$\pm 3.4$	cm
$d_{\zeta_{M9675}}$	-4.1	3.4	$\pm 1.7$	$\pm 1.7$	cm
$d_{\zeta_{M0875}}$	-4.1	5.2	$\pm 1.8$	$\pm 1.8$	cm

$$\text{Bouguer gravity anomaly} \left( \zeta = N - \frac{\Delta g_B}{\gamma} H \right).$$

The second model is the previously used „GUGiK 2001” quasigeoid model.

For this test area, additional calculations were done by increasing the distances between known points. Table 5 includes the basic statistics of the differences  $d_{\zeta_{M075}} = \zeta_{M0} - \zeta_{SL}$ ,  $d_{\zeta_{M9675}} = \zeta_{M96} - \zeta_{SL}$ ,  $d_{\zeta_{M0875}} = \zeta_{M08} - \zeta_{SL}$  for this variant, where distances between adjacent known points are between 53 and 109 km, and the mean distance is about 75 km. The variant encompasses 23 points which are recognised as known data points and 77 unknown test points.

#### 4. DISCUSSION OF THE RESULTS

Analysing the results for the test area P1, one has to notice the very high conformity of the determined height anomalies with the “GUGiK 2001” model. The extreme differences presented in Table 1 do not exceed accuracy of the “GUGiK 2001” quasigeoid model, and the RMS value of mismatch does not exceed  $\pm 7$  mm. Global geopotential models are not very important, which is also worth emphasising here. Application of these models increases modelling accuracy to a very limited degree and that increase is almost the same for both the used global geopotential models.

The fit of the model in question to the POLREF network points for the areas P2 and P3 indicates a high accuracy of the model. The RMS values of  $d_{\zeta_{M96}}$  and  $d_{\zeta_{M08}}$  (Tables 2, 3, 5) do not exceed the mean error of GNSS/levelling data. Comparing the results with relevant accuracy parameters of EGM96 and EGM08 models, one can notice the lack of significant impact of the geopotential model quality on the final result.

The M0 variant (without any global geopotential model) features slightly higher values of all the basic statistics of discrepancy. This decrease of accuracy depends on the distance between the known GNSS/levelling points, and is minor but distinct when the mean distance is approx. 40 - 50 km (Tables 2 and 3) and significant for larger distances (Table 5). This factor indicates clearly the need for using global geopotential models in the calculations.

Table 4 presents the accuracy parameters of models developed with classical methods. Referring to these results, it should be noted that the height anomalies obtained by gravity inversion methodology, based on gravity data in  $5' \times 5'$  grid, in terms of accuracy correspond to height anomalies calculated by the FFT technique based on gravity data with  $1' \times 1'$  resolution. Usage of the same resolution of gravity data ( $5' \times 5'$ ) in both the techniques, shows better results in the gravity inversion technique.

It should also be noted, that in the recent years a number of analyzes of accuracy of global geopotential models for the area of Poland (e.g. Kryński and Łyszkowicz, 2005; Kryński and Kloch-Główka, 2009; Łyszkowicz, 2009a; Łyszkowicz, 2009b) and locally, for the Lower Silesia area (Trojanowicz, 2009) were carried out. The outcomes included in Tables 1, 2 and 3 are consistent with results obtained previously and show a very high accuracy of EGM08 model.

#### 5. CONCLUSIONS

Three examples of local modelling of quasigeoid heights using the gravity data inversion technique have been discussed in this paper. The examples differ in the area under examination and, to some degree, in the nature of the terrain, as well as density of gravity points that have been used for analysis.

On the basis of the results presented, some of the features characterizing the approach may be indicated. First of all, the method itself facilitates local modelling of the quasigeoid height using local data. The method features a small edge effect and for this reason it can be used for small areas, using gravimetric data only from a region for which the quasigeoid model is determined, as well as from its closest surroundings.

In comparison to the established, integral methods, the approach under consideration seems to have significantly smaller requirements with respect to the amount of needed gravity data and resolution of a digital terrain model. That is mainly indicated by the accuracy obtained for the test field P3.

The shortcoming of this method is the need to use the GNSS/levelling height anomalies. In the examples discussed, mean distances between adjacent, known GNSS/levelling points, can be estimated in the range between ca. 30 km (region P1) and ca. 45-52 km (regions P2 and P3). Increasing this distance for the test region P3 to approximately 75 km, would decrease accuracy, mainly for the variant that does not use the global geopotential model. This decrease in accuracy is particularly noticeable for points situated close to the border of the study area. Taking into consideration slightly better modelling results with variants which use global geopotential models, also in the other presented examples, it is sensible to use these models for any quasigeoid modelling using this approach.

#### ACKNOWLEDGEMENTS

The author would like to thank the two reviewers for the constructive comments and suggestions.

#### REFERENCES

- Antunes, C., Pail, R. and Catalao, J.: 2003, Point mass method applied to the regional gravimetric determination of the geoid. *Stud. Geophys. Geod.*, 47, July, 495–509, Prague, Czech Republic.
- Barthelmes, F. and Kautzleben, H.: 1983, A new method of modelling the gravity field of the Earth by point masses. *Proceedings of the XVIII General Assembly of the IUGG*, Hamburg, August, 442–447.
- Barthelmes, F. and Dietrich, R.: 1991, Use of point masses on optimized positions for the approximation of the gravity field. In: *Determination of the Geoid: Present and Future*, Springer, Berlin, 484–493.
- Blakely, R.J.: 1995, *Potential Theory in Gravity and Magnetic Applications*. Cambridge University Press.
- Brovar, W.W.: 1983, Gravity field in problems of engineering geodesy. Science, Moscow.
- Claessens, S.J., Featherstone, W.E. and Barthelmes, F.: 2001, Experiments with point-mass gravity field modelling in the Perth region, Western Australia, *Geomatics Research Australasia*, 75, 53–86.
- Fajkiewicz, Z.: 1972, *An Outline of Applied Geophysics*. Wydawnictwo geologiczne, Warsaw – reference book, (in Polish).
- Featherstone, W.E.: 2000, Refinement of gravimetric geoid using GPS and levelling data, *Journal of Surveying Engineering*, 126(2), 27–56, doi: 10.1061/(ASCE)0733-9453(2000)126:2(27).
- Forsberg, R.: 1984, A study of terrain reductions, density anomalies and geophysical inversion methods in gravity field modelling. *Reports of the Department of Geodetic Science and Surveying*, No. 355. The Ohio State University.
- Forsberg, R. and Tscherning, C.C.: 1997, Topographic effects in gravity field modelling for BVP. *Geodetic Boundary Value Problems in view of the one centimetre geoid*. Lecture notes in earth science, Springer-Verlag Berlin Heidelberg.
- Heck, B.: 2003, Integral Equation Methods in Physical Geodesy. In: Grafarend, E.W., Krumm, F.W., Schwarze, V.S. (Eds.): *Geodesy - The Challenge of the 3rd Millennium*. Springer-Verlag, 197–206.
- Holota, P.: 1997a, Coerciveness of the linear gravimetric boundary-value problem and a geometrical interpretation. *J. Geodesy*, 71, 640–651.
- Holota, P.: 1997b, Variational methods for geodetic boundary value problems. *Geodetic boundary value problems in view of the one centimetre geoid*. Lecture notes in Earth science, Springer-Verlag Berlin Heidelberg.
- Holota, P.: 1999, Variational methods in geoid determination and function bases, *Phys.Chem. Earth (A)*, 24, No.1, 3–14.
- Holota, P.: 2011, Reproducing kernel and Galerkin's matrix for the exterior of an ellipsoid: Application in gravity field studies, *Stud. Geophys. Geod.*, 55 (2011), 397–413.
- Krarup, T.: 1969, A contribution to the mathematical foundation of physical geodesy. *Geodaetisk Institut Meddelese*, No. 44, Copenhagen.
- Królikowski, C. and Polechońska, O.: 2005, Quality of crustal density data in Poland. *Workshop II: Summary of the project on a cm geoid in Poland 16-17 November 2005*, Warsaw.
- Kryński, J.: 2007, Precise quasigeoid modelling in Poland - results and accuracy estimation (in Polish). *Instytut Geodezji i Kartografii, seria monograficzna nr 13*. Warsaw.
- Kryński, J. and Kloch-Główka, G.: 2009, Evaluation of the performance of the new EGM08 global geopotential model over Poland, *Geoinformation Issues*, 1, No 1, Warsaw, 7–17.
- Kryński, J. and Lyszkowicz, A.: 2005, Study on choice of global geopotential model for quasigeoid determination in Poland, *Geodezja i Kartografia*, 54, No 1, 17–36.
- Kryński, J., Osada, E. and Figurski, M.: 2005, GPS/levelling data in Poland in view of precise geoid modelling. *Workshop II: Summary of the project on a cm geoid in Poland 16–17 November 2005*, Warsaw.
- Lehmann, R.: 1995, Gravity field approximation using point masses in free depths. *Bulletin 1 of IAG* 129–140.
- Lemoine, F.G., Kenyon, S.C., Factor, J.K., Trimmer, R.G., Pavlis, N.K., Chinn, D.S., Cox, C.M., Klosko, S.M., Luthcke, S.B., Torrence, M.H., Wang, Y.M., Williamson, R.G., Pavlis, E.C., Rapp, R.H. and Olson, T.R.: 1998, *The Development of the Joint NASA GSFC and NIMA Geopotential Model EGM96*. NASA Goddard Space Flight Center, Greenbelt, Maryland, 20771 USA, July 1998.
- Li, Y. and Oldenburg, D.W.: 1998, 3-D inversion of gravity data. *Geophysics* 63, No. 1, 109–119.

- Lyszkowicz, A.: 1993, The geoid for the area of Poland, *Artificial Satellites*, 28, No 2, Planetary Geodesy No 19, 75–150, Warsaw.
- Lyszkowicz, A.: 1998, The Polish gravimetric quasi-geoid QGEOID97 versus vertical reference system Kronsztad 86, Reports of the Finish Geodetic Institute, 98, 4.
- Lyszkowicz, A.: 2000, Improvement of the quasigeoid model in Poland by GPS and levelling data, *Artificial Satellites, Journal of Planetary Geodesy*, 35, No 1, 3–8.
- Lyszkowicz, A.: 2009a, Accuracy evaluation of quasi-geoid from EGM08 model for area of Poland, *Acta Sci. Pol. Geod. Descr. Terr.*, 8(4), 39–47.
- Lyszkowicz, A.: 2009b, Assessment of accuracy of EGM08 model over the area of Poland, *Technical Sciences*, Nr 12, UWM, Olsztyn.
- Lyszkowicz, A. and Denker, H.: 1994, Computation of gravimetric geoid for Poland using FFT, *Artificial Satellites*, 29, No 1, Planetary Geodesy No 21, 1–11. Warszawa
- Lyszkowicz, A. and Forsberg, R.: 1995, Gravimetric geoid for Poland area using spherical FFT, *IAG Bulletin d'Information No 77, IGES Bulletin No 4, Special Issue*, Milan, 153–161.
- Moritz, H.: 1972, Advanced least-squares methods. Reports of the Department of Geodetic Science and Surveying, No. 175. The Ohio State University.
- Nagy, D.: 1966, The gravitational attraction of right angular prism. *Geophysics*, 31, 362–371.
- Nagy, D., Papp, G. and Benedek, J.: 2001, The gravitational potential and its derivatives for the prism. *Journal of Geodesy* 74, 552–560.
- Osada, E., Krynski, J. and Owczarek, M.: 2005, A robust method of quasigeoid modelling in Poland based on GPS/levelling data with support of gravity data, *Geodezja i Kartografia*, 54, No 3, 99–117.
- Pavlis, N.K., Holmes, S.A., Kenyon, S.C. and Factor, J.K.: 2008, An Earth gravitational model to degree 2160: EGM2008. EGU General Assembly 2008 Vienna, Austria, April 13–18,
- Pażus, R., Osada, E. and Olejnik, S.: 2002 The levelling geoid 2001. *Magazyn Geoinformacyjny Geodeta*, Nr 5(84), maj 2002, (in Polish).
- Tarantola, A.: 2005, *Inverse Problem Theory and Methods for Model Parameter Estimation*. Society for Industrial and Applied Mathematics, Philadelphia.
- Telford, W.M., Geldart, L.P. and Sheriff, R.E.: 1990, *Applied Geophysics* Second Edition. Cambridge University Press – reference book.
- Trojanowicz, M.: 2002, Local modelling of the disturbing potential with the use of quasigeoid heights, gravimetric data and digital terrain model. *Geodesy and Cartography*, LI, 1-2, 35–43.
- Trojanowicz, M.: 2007, Local modeling of quasi-geoid heights on the strength of the unreduced gravity and GPS/leveling data, with the simultaneous estimation of topographic masses density distribution. *Electronic Journal of Polish Agricultural Universities*, 10 (4) 35, topic Geodesy and Cartography. <http://www.ejpau.media.pl/articles/volume10/issue4/art-35.pdf>
- Trojanowicz, M.: 2009, Estimation of an accuracy of global geopotential models EGM96 and EGM08 at Lower Silesia area. *Acta Sci. Pol. Geod. Descr. Terr.*, 8(1), 19–30, (in Polish).
- Trojanowicz, M.: 2012, Local quasigeoid modelling using gravity data inversion technique - analysis of the fixed coefficients of density model weighting matrix. Paper submitted to *Acta Geodyn. Geomater.* 9, No. 3 (167)..
- Tscherning, C.C.: 2001, Geoid determination after first satellite gravity missions. Paper prepared at the occasion of the 70 birthday of Wolfgang Torge.
- Vajda, P. and Vaniček, P.: 1997, On gravity inversion for point mass anomalies by means of the truncated geoid. *Studia Geophysica et Geodaetica* 41, 329–344
- Vajda, P. and Vaniček, P.: 1999, Truncated geoid and gravity inversion for one point-mass anomaly. *Journal of Geodesy*, 73, 58–66, Springer-Verlag.
- Vajda, P. and Vaniček, P.: 2002, The 3-D truncation filtering methodology defined for planar and spherical models: interpreting gravity data generated by point masses. *Stud. Geophys. Geod.*, 46, 469–484, Prague.